

Modeling ray displacement in addition to ray deviation for 3D BOS

FRANÇOIS NICOLAS^{1,*}, FRÉDÉRIC CHAMPAGNAT², GUY LE BESNERAIS², AND DAVID DONJAT¹

¹ONERA, DMAE, 2 Avenue Edouard Belin, 31400 Toulouse, FRANCE

²ONERA, DTIM, Chemin de la Hunière, 91123 Palaiseau, FRANCE

*Corresponding author: francois.nicolas@onera.fr

Compiled July 22, 2016

We propose a new formulation of the background oriented schlieren problem, relating directly density to image displacements. Reconstruction of a 3D density volume using this model avoids some arbitrary choices of the original approach and leads to a reduction of the biases when high density gradients are encountered.

© 2016 Optical Society of America

OCIS codes: 080.5692 Ray trajectories in inhomogeneous media, 100.3190 Inverse problems, 100.6950 Tomographic image processing.

<http://dx.doi.org/10.1364/ao.XX.XXXXXX>

Eikonal equation describes the light rays path through an inhomogeneous optical index media. Several optical techniques make use of this relation to visualize or measure the density. Among them, background oriented schlieren (BOS) relies on measurement of the displacements of patterns between images recorded with and without the fluid under study [1, 2]. BOS measurement with various orientations can be exploited to reconstruct the density field of the flow. However, while the basic observables are displacements, such 3D BOS reconstruction is always formulated as the numerical inversion of an equation relating density or density gradients to deviations. Ray deviations have to be inferred from displacements, but the mapping is many to one, and additional assumptions are required, such as far field conditions [1] or a priori knowledge on the geometry of the flow [3–5].

The validity of such assumptions is questionable in case of unsteady compressible flows. This letter deals with an alternative formulation of the BOS problem that completely removes the necessity of such hypotheses. It is based on a derivation of the light propagation within an inhomogeneous refractive index volume which accounts for the displacement of the ray together with its deviation.

First, the problem statement is described through Fig. 1 which illustrates the basic setting of BOS. A ray issued from a point H^* of the background inputs the volume under study at some point I_{in}^* , is deviated by density inhomogeneities and exits the volume at I_{out} before striking the camera. The ray deviation is the difference of the direction vectors between the input and

output rays $\epsilon = d_{out} - d_{in}$.

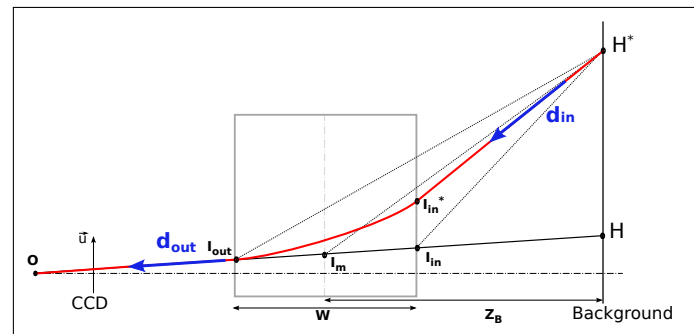


Fig. 1. Basic model for BOS: reference point definition for deviation calculation.

Prolongating the output ray towards the background leads to point H , which is the point from which the light seems to come when the perturbing flow is present. In the reference image without the flow, the light actually comes from H^* . Image correlation techniques are used to match these two regions between the reference and perturbed images. For convenience only points and displacements within the background plane will be considered in the sequel. It does not imply any approximation or loss of generality since there is a one-to-one mapping between the background plane and the image plane. In an ideal situation this mapping is only a scaling, more generally a plane homography, whose parameters are defined by a preliminary calibration of the set-up.

As a result, image measurements give access to the locations of I_{out} , H and H^* and also to the direction vector d_{out} , but neither d_{in} or ϵ is observed. The direction vector d_{in} depends on the input point I_{in}^* which is not known. As they aim at estimating density from deviations, all BOS techniques overcome this issue by using an approximate propagation model where the deflection occurs on some point of the intersection of non perturbed ray OH and the experimental volume. A common choice is the middle point I_m (see Fig. 1) [1, 3].

We will show in the following that such a choice can be rigorously justified for an axisymmetric flow under a paraxial approximation. In other situations, though, it can be a good approximation if the size W of the flow under study is small with

respect to its mean distance to the background. For near field situations, van Hinsberg and Rösgen have proposed a correction factor based on the flow geometry [4]. However, in the general non axisymmetric case, all these geometrical models are prone to bias, because the real deviation is determined by the location of the input point I_{in}^* which, itself, depends on the refraction index field inside the volume. Our goal is to propose a novel propagation model which explains both the deviation and the displacement of the ray, thus providing a rigorous answer to the problem by allowing the formulation of a forward model relating directly density to displacement.

In the following, we mathematically describe this forward model. Our starting point is the Gladstone-Dale relation. This relation states that optical index and density are related through

$$n = 1 + G\rho \quad (1)$$

where G is the Gladstone-Dale constant characterizing the fluid. We assume that G is known so that n and ρ are equivalent descriptions of the flow as regards ray propagation.

We now derive the main equations relating input rays to output rays in terms of both deviation angle and displacement. Our derivations are based on the paraxial approximation of the eikonal equation. Note that, while most previous reference in the BOS community focused on deviation, Stam and Languénou [6] have studied the propagation in terms of ray displacement.

For modeling purposes it is more convenient to propagate rays from the camera toward the background, therefore, in the following figures, direction vectors are represented pointing in the opposite direction with respect to the imaging process.

Let's consider a light ray exiting the camera and propagating through volume of non constant optical index. We define a ray trajectory by a function $\mathbf{x}(s)$ from \mathbb{R} to \mathbb{R}^3 , where s is the curvilinear abscissa. We also write $\dot{\mathbf{x}} \stackrel{\Delta}{=} \frac{d\mathbf{x}}{ds}$ such as:

$$\|\dot{\mathbf{x}}\| = \left\| \frac{d\mathbf{x}}{ds} \right\| = 1 \quad (2)$$

Let us denote by s_{in} the curvilinear abscissa of the entering point I_{in} . The deviation ϵ occurring between s_{in} and an arbitrary position s on the ray trajectory is written :

$$\epsilon(s) = \dot{\mathbf{x}}(s) - \dot{\mathbf{x}}(s_{in}) \quad (3)$$

Our derivations are based on the eikonal equation that describes the ray propagation into an inhomogenous optical index media:

$$\frac{d}{ds} \left(n \frac{d}{ds} \mathbf{x}(s) \right) = \nabla n \quad (4)$$

It can be integrated as follow:

$$\dot{\mathbf{x}}(s) = \frac{1}{n(\mathbf{x}(s))} \int_{s_{in}}^s \nabla n(\mathbf{x}(r)) dr + \frac{n_{in}}{n(\mathbf{x}(s))} \dot{\mathbf{x}}(s_{in}) \quad (5)$$

The previous equation can be simplified considering small optical index variations. In aerodynamic studies, a typical order of G is 10^{-4} , whereas the range of ρ does not exceed 10 kg.m^{-3} even in the case of shockwaves. In this case, according to (1), the relative range of variation for the optical index does not exceed 10^{-3} and the following approximation of (5) holds:

$$\dot{\mathbf{x}}(s) \approx \frac{1}{n_{in}} \int_{s_{in}}^s \nabla n(\mathbf{x}(r)) dr + \dot{\mathbf{x}}(s_{in}) \quad (6)$$

Integrate again the previous equation leads to the displacement:

$$\mathbf{x}(s) - \mathbf{x}(s_{in}) \approx \frac{1}{n_{in}} \int_{s_{in}}^s dt \int_{s_{in}}^t \nabla n(\mathbf{x}(r)) dr + (s - s_{in}) \dot{\mathbf{x}}(s_{in}) \quad (7)$$

Finally, by integrating by part:

$$\mathbf{x}(s) - \mathbf{x}(s_{in}) \approx \frac{1}{n_{in}} \int_{s_{in}}^s (s - t) \nabla n(\mathbf{x}(t)) dt + (s - s_{in}) \dot{\mathbf{x}}(s_{in}) \quad (8)$$

Finally, we classically consider the paraxial approximation. Under this assumption, the previous integrals can be evaluated on straight rays rather than on the real curved ones. This approximation has been checked to be accurate with a relative error less than 0.01% on the test case presented below. It is also more general than the nearly parallel ray approximations of Merzkirch [7] and Dalziel [1].

We then replace, in the previous equations, $\mathbf{x}(s)$ by $\mathbf{x}_0(s)$ where $_0$ denotes the paraxial ray:

$$\mathbf{x}_0(s) = \mathbf{x}(s_{in}) + (s - s_{in}) \dot{\mathbf{x}}(s_{in}) \quad (9)$$

From (3) and (6) we derive the classical BOS equation for ray deviation [3]:

$$\epsilon(s_{out}) \approx \frac{1}{n_{in}} \int_{s_{in}}^{s_{out}} \nabla n(\mathbf{x}_0(s)) ds \quad (10)$$

From ray deviation one derives the ray displacement Δ defined as the difference between the exit point from the volume and the one corresponding to the paraxial ray:

$$\Delta \stackrel{\Delta}{=} \mathbf{x}(s_{out}) - (\mathbf{x}(s_0) + (s_{out} - s_0) \dot{\mathbf{x}}(s_0)) \quad (11)$$

Combining this definition and (8) yields

$$\Delta \approx \frac{1}{n_{in}} \int_{s_{in}}^{s_{out}} (s_{out} - t) \nabla n(\mathbf{x}_0(t)) dt \quad (12)$$

which is reminiscent of Eq. (7) in [6].

So thanks to the paraxial approximation, the mapping from input ray to output ray is linear with respect to the optical index n . By the Gladstone-Dale relation (1) it is also linear with respect to ρ , so

$$\boxed{\epsilon(\rho) \approx \frac{G}{n_{in}} \int_{s_{in}}^{s_{out}} \nabla \rho(\mathbf{x}_0(s)) ds} \quad (13)$$

$$\boxed{\Delta(\rho) \approx \frac{G}{n_{in}} \int_{s_{in}}^{s_{out}} (s_{out} - t) \nabla \rho(\mathbf{x}_0(t)) dt} \quad (14)$$

where the dependence of ϵ and Δ with respect to ρ is underlined.

At this point, we have expressed a new formulation of the forward model for light ray propagation, relating density to displacement. Before deriving a new 3D BOS algorithm based on this model, we further analyze the classical approach [3].

Classical 3D BOS methodology is to minimize

$$\|\epsilon_m - \epsilon(\rho)\|^2 \quad (15)$$

where the deviation measurements ϵ_m are obtained by assuming that the input and output rays cross at midpoint I_m , as illustrated in the upper part of Fig. 2.

Such an approximation is rigorously justified hereafter for an axisymmetric flow. In this case, the paraxial ray crosses a circle

and the function $\nabla\rho(\mathbf{x}_0(s))$ becomes symmetric between s_{in} and s_{out} . Using symmetry, one gets

$$\int_{s_{in}}^{s_{out}} (s_{out} - r) \nabla\rho(\mathbf{x}_0(r)) dr = \int_{s_{in}}^{s_{out}} (r - s_{in}) \nabla\rho(\mathbf{x}_0(r)) dr = \frac{\Delta n_{in}}{G}. \quad (16)$$

Using (13) the sum of the two leftmost terms of (16) identifies with $n_{in}(s_{out} - s_{in})\epsilon/G$, and we obtain

$$2\Delta = (s_{out} - s_{in})\epsilon. \quad (17)$$

This equality means exactly that the paraxial ray and the deviated ray intersect at the midpoint between I_{in} and I_{out} .

In the general case, axisymmetry does not hold and the previous assumption can lead to a high bias on the reconstruction especially when the width of the schlieren object W , is not negligible with respect to the distance to the background Z_B .

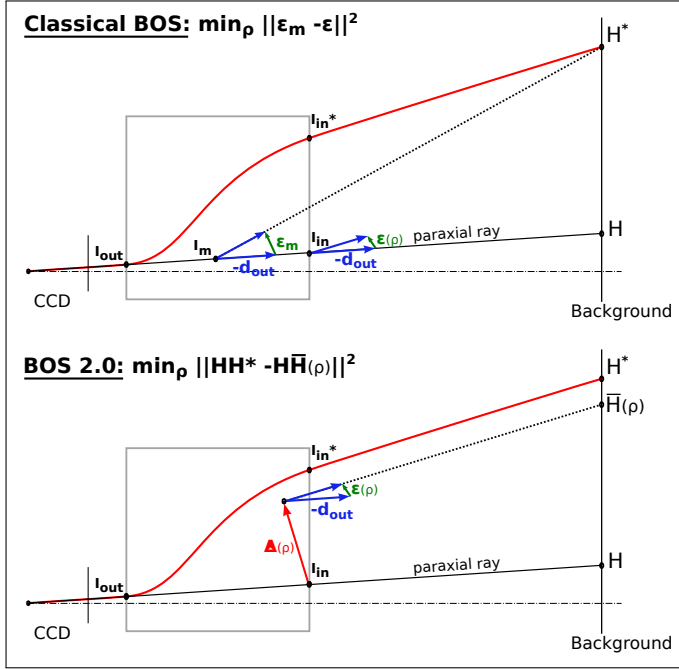


Fig. 2. Sketch of the forward models involved in classic BOS (upper part) and in the proposed BOS 2.0

Considering our new forward model, we are now able to predict the light ray displacement $\Delta(\rho)$ occurring inside the volume under study. As sketched in the lower part of Fig. 2 one can predict the final displacement $H\bar{H}(\rho)$ by projecting the point $I_{in} + \Delta(\rho)$ onto the background with respect to the direction $-d_{out} + \epsilon(\rho)$.

This projection is straightforward given the equation of the background plane. Yet, for the purpose of inversion, it is more efficient to use a linear approximation whose computation is also straightforward. For the sake of simplicity we identify hereafter $H\bar{H}(\rho)$ with its linear approximation. Then, ρ being known, one is able to accurately predict the measured displacement HH^* and a new BOS 2.0 method can be defined as searching for ρ which minimizes:

$$\|HH^* - H\bar{H}(\rho)\|^2. \quad (18)$$

Let us remark that such a methodology does not require any prior knowledge of the flow topology and does not depend on a geometrical model of the working volume in contrast with the formulation of classic BOS [1, 3] or further refinements [4, 5].

We describe hereafter a numerical approach for practical solving of the BOS 2.0 problem by discretization of the objective function (18). This approach is used in the next paragraph to assess the pertinence of the proposed BOS 2.0 method.

The density field ρ is defined over a volume \mathcal{V} and is discretized on a piecewise constant "voxel" basis. The vector of coefficients of ρ on this discrete representation is denoted ρ . On the camera plane, pixel discretisation defines a finite set of direction vectors d_{out} that are mapped onto a set of displacements δ on the background plane. This one-to-one mapping derives from the calibration of the BOS setting [8]. The full forward problem can now be cast in matrix form:

$$\delta = B\rho = P \begin{pmatrix} T & T & T \\ T^2 & T^2 & T^2 \end{pmatrix} \begin{pmatrix} D_x \\ D_y \\ D_z \end{pmatrix} \rho \quad (19)$$

The observation matrix B is decomposed into three operators. The rightmost one computes density gradients using a finite difference matrix D_w along each direction $w \in \{x, y, z\}$. We use a second-order central difference scheme and, as regard boundary conditions, a reference density ρ_{out} is set outside \mathcal{V} . The central matrix is the tomographic integration of density gradients, which provides deviation (upper row) and displacement (lower row). T performs integration by summing density gradients over discretized rays (discretization step is typically 1/10 of a voxel) leading to deviations. Displacements are computed as the cumulative sum of deviations, hence the corresponding operator is denoted T^2 . Finally, the leftmost operator P encodes the linearized projection of point $I_{in} + \Delta(\rho)$ (see Fig. 2) onto the background.

As a combination of tomographic integrations and gradient operators, B matrix is ill-conditioned. Some regularization strategy is needed, we choose to simply penalize the data term with the L_2 norm of the density spatial gradient as in [5]. The solution is then defined as the minimizer of the following compound criterion:

$$\mathcal{J}(\rho) = \|B\rho - \delta\|^2 + \lambda \|\bar{D}\rho\|^2, \quad (20)$$

where \bar{D} is a forward difference gradient operator. The balance between both terms is set by the regularization parameter $\lambda > 0$. This well-behaved quadratic criterion reduces the effect of the noise but tends to oversmooth the density discontinuities that may be present in the flow. Other, more sophisticated, regularization terms could be used here, but are outside the scope of this paper.

Minimization of (20) is performed using a conjugate gradient iterative algorithm as in [5]. Final convergence is obtained when the gradient of the criteria (20) reaches a stopping value equals to 10^{-16} .

To illustrate the pertinence of the BOS 2.0 approach we apply a 2D version of our algorithm implemented in Matlab. In order to be more representative, we have selected an application case derived from a fluid mechanics. This reference instantaneous density field is extracted from a LES simulation of a supersonic jet. The jet is issued from a convergent nozzle with a Nozzle Pressure Ratio (Total pressure / Ambient pressure) NPR=2.2736. One transverse slice of dimensions 50x50 cm is chosen at a cell-shock location. It is discretized on a regular grid of 100×100 2D voxels. The density field, shown on the leftmost image of Fig. 3 presents a large diversity of density gradients including

representative turbulence scale. 12 virtual cameras are located around the density field on half a ring at a distance of 1.5 m from the flow center. Each camera has 100 pixels and is modeled as a pinhole. Finally, 12 virtual backgrounds face the cameras, 3 m away from them.

First, we generate the true displacement field associated with each camera using a 4th order Runge-Kutta integration of the eikonal equation. Deviation data, associated to the classical BOS reconstruction, are then generated from the displacements using the midpoint assumption. No noise is added to the data, as we intend here to validate the forward model rather than the inversion method.

The reconstruction is performed on the same discretization as the input volume (*i.e.* 100 × 100 voxels) and takes about 200 iterations to converge. We present on Fig. 3 the ground truth density field (on the left), the reconstruction obtained with classical BOS (in the middle) and the BOS 2.0 result (on the right). The regularization parameters have been chosen to yields the same amount of smoothing for both methods, but essentially improves the convergence as this is a noiseless case. The flow topology is well recovered both for classical BOS and BOS 2.0. Obviously, the fine scale turbulence is smoothed out due to the limited number of data but the main shape of the shock cell is well defined. Comparing both reconstructions it appears that classical BOS significantly overestimates density levels whereas BOS 2.0 is able to reconstruct right levels. As a consequence, BOS 2.0 reaches a much better RMS error than classical BOS.

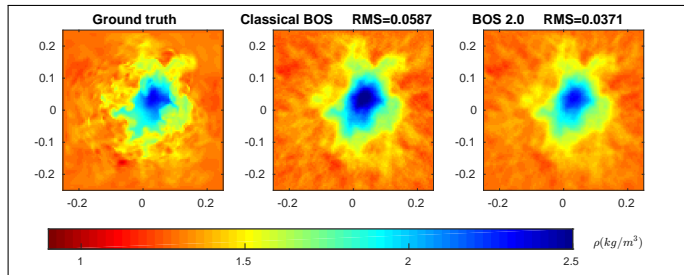


Fig. 3. Ground truth (left) and reconstructed density fields by classical BOS (middle) and BOS 2.0 (right), with the associated root-mean-squared errors (RMS).

Looking at horizontal and vertical slices on Fig. 4 shows that the overestimation of the density level in the classical BOS reconstruction is further exacerbated by the strong density gradients. In contrast, BOS 2.0 recovers the right level with the same amount of smoothing.

In this paper, we have introduced a new formulation of BOS based on a model of propagation of light rays through inhomogeneous index media. This model provides not only the deviation but also the displacement of the ray occurring inside the schlieren object. Our BOS 2.0 formulation relates directly the density field to the background displacements and avoids arbitrary choices required in classical BOS to convert measured displacement to deviation. We then derive a 3D BOS reconstruction algorithm based on the minimization of a goodness-to-fit criterion written in terms of displacement measurement. A 2D version of the algorithm has been implemented in Matlab and tested on a representative fluid mechanics case. The algorithm shows a good performance for reconstructing the flow topology. Above all, the new BOS 2.0 algorithm is not subject to the biases

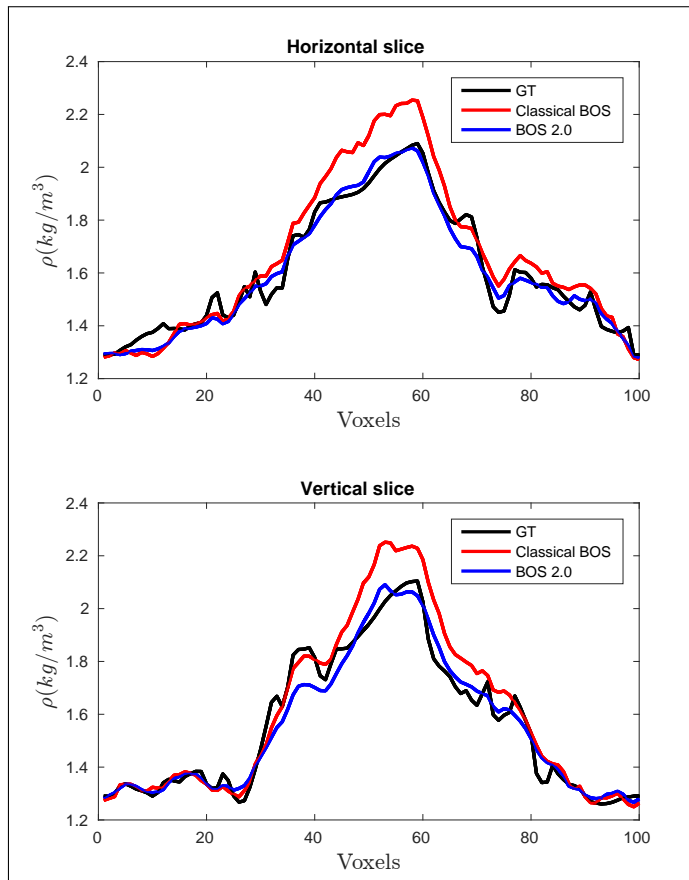


Fig. 4. Horizontal(left) and vertical(right) slices of the reconstructed density fields as compared to the ground truth.

on the density levels which are observed in classical BOS. This property is essential for 3D BOS reconstruction of instantaneous density fields, especially for aerothermal applications where the estimation of temperature fields is required.

ACKNOWLEDGEMENTS

The authors want to thank G. Daviller from Cefracs for providing the LES simulation of the supersonic jet.

REFERENCES

1. S. B. Dalziel, G. O. Hughes, and B. R. Sutherland, *Exp Fluids* **28**, 322 (2000).
2. M. Raffel, *Experiments in Fluids* **56**, 1 (2015).
3. B. Atcheson, I. Ihrke, W. Heidrich, A. Tevs, D. Bradley, M. Magnor, and H.-P. Seidel, "Time-resolved 3D capture of non-stationary gas flows," in "ACM transactions on graphics (TOG)," , vol. 27 (ACM, 2008), vol. 27, p. 132.
4. N. van Hinsberg and T. Rösgen, *Experiments in Fluids* **55**, 1 (2014).
5. F. Nicolas, V. Todoroff, A. Plyer, G. Le Besnerais, D. Donnat, F. Micheli, F. Champagnat, P. Cornic, and Y. Le Sant, *Experiments in Fluids* **57**, 1 (2016).
6. J. Stam and E. Languénou, "Ray tracing in non-constant media," in "Rendering Techniques '96," X. Pueyo and P. Schröder, eds. (Springer Vienna, 1996), Eurographics, pp. 225–234.
7. W. Merzkirch, *Flow visualization* (Elsevier, 2012).
8. Y. Le Sant, V. Todoroff, A. Bernard-Brunel, G. Le Besnerais, F. Micheli, and D. Donnat, "Multi-camera calibration for 3DBOS," in "17th Int. Symp. on Applications of Laser Techniques to Fluid Mechanics," (2014).

FULL REFERENCES

1. S. B. Dalziel, G. O. Hughes, and B. R. Sutherland, "Whole-field density measurements by 'synthetic schlieren,'" *Exp Fluids* **28**, 322–335 (2000).
2. M. Raffel, "Background-oriented schlieren (BOS) techniques," *Experiments in Fluids* **56**, 1–17 (2015).
3. B. Atcheson, I. Ihrke, W. Heidrich, A. Tevs, D. Bradley, M. Magnor, and H.-P. Seidel, "Time-resolved 3D capture of non-stationary gas flows," in "ACM transactions on graphics (TOG)," , vol. 27 (ACM, 2008), vol. 27, p. 132.
4. N. van Hinsberg and T. Rösgen, "Density measurements using near-field background-oriented schlieren," *Experiments in Fluids* **55**, 1–11 (2014).
5. F. Nicolas, V. Todoroff, A. Plyer, G. Le Besnerais, D. Donjat, F. Micheli, F. Champagnat, P. Cornic, and Y. Le Sant, "A direct approach for instantaneous 3D density field reconstruction from background-oriented schlieren (BOS) measurements," *Experiments in Fluids* **57**, 1–21 (2016).
6. J. Stam and E. Languénou, "Ray tracing in non-constant media," in "Rendering Techniques '96," X. Pueyo and P. Schröder, eds. (Springer Vienna, 1996), Eurographics, pp. 225–234.
7. W. Merzkirch, *Flow visualization* (Elsevier, 2012).
8. Y. Le Sant, V. Todoroff, A. Bernard-Brunel, G. Le Besnerais, F. Micheli, and D. Donjat, "Multi-camera calibration for 3DBOS," in "17th Int. Symp. on Applications of Laser Techniques to Fluid Mechanics," (2014).